A Comparison Between Adaptive Kernel Density Estimation and Gaussian Mixture Regression for Real-Time Tumour Motion Prediction from External Surface Motion

F. Tahavori, *Student Member, IEEE,* M. Alnowami, and K. Wells

***Abstract*—In this present study, tumour (3D) locations are predicted via external surface motion, extracted from abdomen/thoracic surface measurements that can be used to enhance dose targeting in external beam radiotherapy. Canonical Correlation Analysis (CCA) is applied to the surface and tumour motion data to maximise the correlation between them. This correlation is exploited for motion prediction [1]. Nine dynamic CT datasets were used to extract the surface and tumour motion and to create the Canonical Correlation model (CCM). Gaussian Mixture Regression (GMR) and Adaptive Kernel Density Estimation (AKDE) were trained on these nine datasets to predict the respiratory signal by updating the surface motion and CCM. A leave-one-out method was used to evaluate and compare the performance of GMR and AKDE in predicting the tumour motion.**

***Index Terms*—Tumour prediction, Canonical Correlation Analysis, CT datasets, Adaptive Kernel Density Estimation, Gaussian Mixture Regression.**

I. Introduction

RESPIRATORY motion induces uncertainty in Image-Guided Radiation Therapy (IGRT) and Intensity-Modulated Radiation Therapy (IMRT), can results in sub-optimal dose delivery to the target or normal tissue [2]. Respiratory motion is also a source of degradation in Positron Emission Tomography (PET), where movement can adversely affect subsequent clinical diagnosis such as the position and extent of a tumour [3].

Motion correction can be used to address these issues. For radiotherapy, the tumour position can be imaged and tracked directly using fluoroscopic images. However, in vivo tumour tracking is not applicable in certain situations. As an alternative, implanted fiducial marker in the tumour or host organs has been used as a surrogate to enhance identification of tumour position [4]. Several studies have used gold fiducial markers that are detectable under x-ray illumination. The application of implanted markers is however limited due to their invasive nature and the increased risk of pneumothorax [5].

To decrease the additional dose from radiographic imaging, episodic imaging can be combined with measurement of the external breathing signal to construct a correlation model. During treatment this model can be used to estimate tumour position. Beddar et al. proposed to use the correlation between the motion of an external marker and internal fiducials implanted in the liver [6]. However, most studies suggest that the correlation is non-stationary and there is a lag time between image acquision, processing and dose delivery. To address these issues, predictions models based on observed anterior respiratory signal are now gaining significant interest [4].

The primary aim of this study is to generate a patient specific prediction model to predict the 3D future position of the tumour based upon the predicted position of a surrogate signal. By predicting the position of the anterior abdominal/thoracic surface, the correlation between this estimated future surrogate position and the future tumour position can be made via a CCM. In this work, the performances of two different prediction models are compared: Adaptive Kernel Density Estimation (AKDE) and Gaussian Mixture Regression (GMR), using a leave-one-out cross-validation to evaluate performance. In doing so, nine dynamic CT datasets of patients with lung cancer were used. Their surface and tumour position were extracted. The AKDE and GMR were trained on these datasets to estimate the future position of anterior surface. In addition, the CCM model is created by these datasets to map external and internal motion.

II. Methodology and Preliminary Results

A. Methodology

In the present study, the external surface motion is observed by extracting the chest surface from dynamic CT data. Principal Component Analysis (PCA) is applied to the external surface motion data to project it to a lower dimension.

Tumour volume was calculated through segmentation and labeling of tumour lesions in each phase of the dynamic CT data using ITK-SNAP [7]. The motion of the tumour's centre of gravity is then tracked in each phase. CCA is then used to find two basis vectors for tumour motion $(\mathbf{u})$ and external surface motion $(\mathbf{v})$ such that the correlation between data

Manuscript received November 16, 2012.

F. Tahavori is with the Centre for Vision, Speech and Signal Processing, Faculty of Engineering and Physical Sciences, University of Surrey, Guildford, Surrey GU2 7XH, UK (telephone: +44 1483 689865, e-mail: fatemeh.tahavori@surrey.ac.uk).

M. Alnowami is with the Centre for Vision, Speech and Signal Processing, Faculty of Engineering and Physical Sciences, University of Surrey, Guildford, Surrey GU2 7XH, UK.

K. Wells is with the Centre for Vision, Speech and Signal Processing, Faculty of Engineering and Physical Sciences, University of Surrey, Guildford, Surrey GU2 7XH, UK.

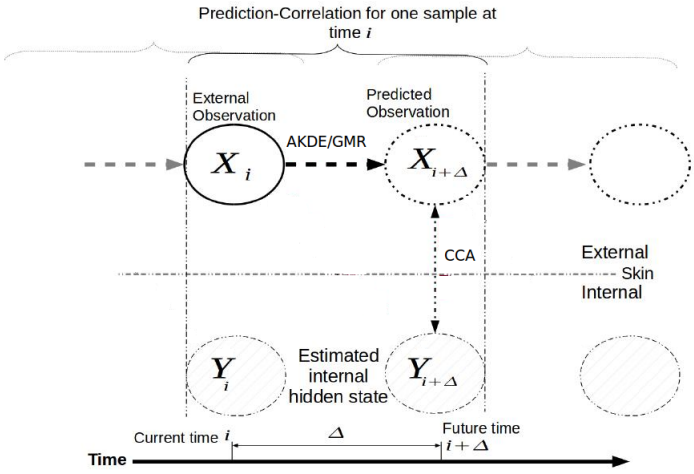

Fig. 1: A schematic process of prediction-correlation model for predicting the future position of the tumour via anterior external surface as a surrogate. Where X_i and Y_i are the anterior surface position surrogate and the internal tumour position respectively. Also, $X_{i+\Delta}$ and $Y_{i+\Delta}$ are the estimated of the external surface and internal tumour position.

projections on these vectors is maximized. Finally, a GMR and AKDE models are trained on the data to estimate the position of the lung tumour with the external thoracic and abdomen surface as a surrogate.

Figure 1 illustrates a schematic process of prediction-correlation model for predicting the future position of the tumour via anterior external surface as a surrogate. As can be seen in Figure 1, the future position of the anterior surface is obtained using AKDE and GMR and their results will be used in a correlation step where the future position of the internal tumour is predicted using a CCM model.

B. Data

Table I presents the characteristics of nine patients 4D CT image with lung cancer used in this study. Each dataset comprises ten phases of a 3D CT volume during one average respiratory cycle. These datasets were collected from different sources. Datasets 1-5 were acquired using a helical 4D CT system located at the Lon Brard Cancer Center [8]. Datasets 6-8 were acquired on a cine 4D CT system located in the MD Anderson Cancer Center [9]. The 9th dataset was a cine 4D CT from Royal Surrey Country Hospital.

C. External Surface Motion

No external tracker signal was available thus the CT datasets themselves were used to extract their own respective surfaces information. Intensity thresholding was followed by edge detection to extract the anterior surface motion. The steps are described in Figure 2. Firstly each trans-axial slice of a dynamic CT data volume was truncated to include only the abdominal/thoracic surface. Each image was then converted to binary form to illustrate clearly the edge of the upper skin surface from the background.

TABLE I: The parameters and characteristic of dynamic CT data where each dataset comprises ten phases of a 3D CT volume during one average respiratory cycle.

No.Data	Data Dimension	Voxel Size (mm)	# Voxel	Lesion size(mm^3)
1	512×512×141	0.976×0.976×2.0	4678	8922.58
2	512×512×169	0.976×0.976×2.0	1020	1945.50
3	512×512×187	0.782×0.782×2.0	1272	1552.80
4	512×512×181	1.172×1.172×2.0	288	791.02
5	512×512×161	1.172×1.172×2.0	2017	5539.86
6	512×512×128	0.970×0.970×2.5	2785	6551.02
7	512×512×128	0.970×0.970×2.5	355	835.05
8	512×512×120	0.970×0.970×2.5	16816	39555.40
9	512×512×112	0.976×0.976×2.5	17952	42800.90

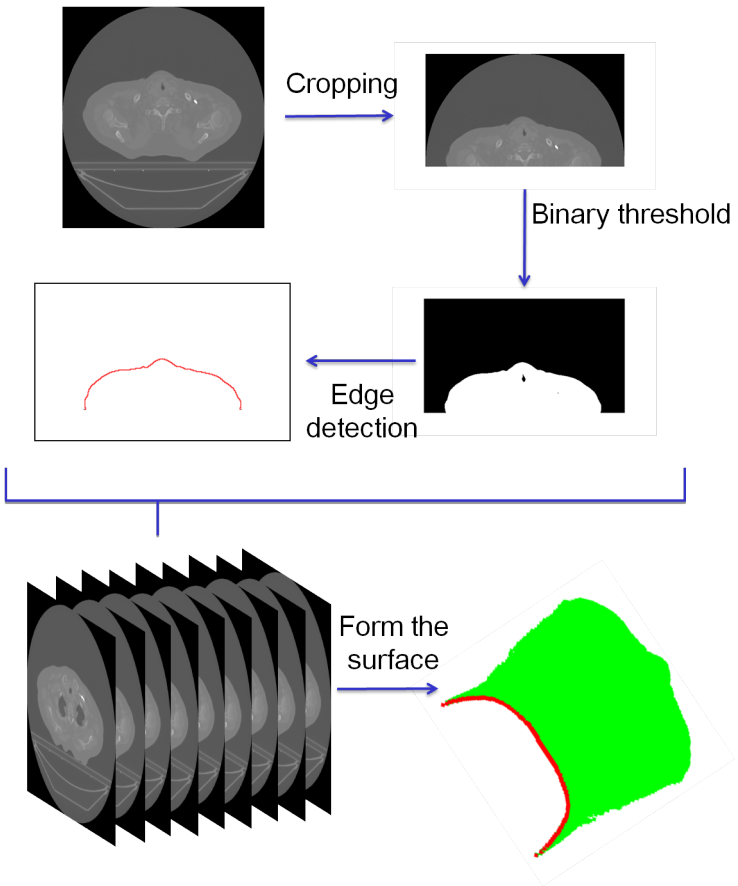

Fig. 2: Steps for extracting a marker-less external surface motion from dynamic CT-datasets.

The edge-detector was used to obtain all pixels coordinates on the outer contour that cover the upper skin surface of each slice to obtain the whole body anterior surface. Control points were used to interpolate from these surfaces. These points were used to reduce dimensionality. This process was repeated across all phases in the dynamic dataset, to track the surface motion. Pixel spacing and slice thickness information were utilized along with the points to create real world dimensions of motion. Two patches were allocated onto the abdominal and thoracic surfaces. Figure 3 illustrates the external surface that is divided into two sections, thoracic ($\mathbf{s^{(T)}}$) and abdomen regions ($\mathbf{s^{(A)}}$). The thoracic motion sequences were arranged

as a vector $\mathbf{s_n^{(T)}}$ ($\mathbf{s_n^{(A)}}$ has similar structure):

$$\mathbf{s_n^{(T)}} = [x_{n,1}, y_{n,1}, z_{n,1}, ..., x_{n,p}, y_{n,p}, z_{n,p}]^T, \quad (1)$$

where $x_{n,1}, y_{n,1}, z_{n,1}, ..., x_{n,p}, y_{n,p}, z_{n,p}$ are the Cartesian coordinates of each pixel in phase n and p is number of voxel on the surface. PCA was applied to project the extracted motion into a lower dimensional subspace. These signals will be used in the CCM to measure the correlation of each section with the internal tumour.

D. Tumour Motion

Tumour motion in the lungs was extracted from the nine patients' dynamic CT datasets as follows: Firstly, the tumour volume was segmented manually and labeled for each phase as can be seen in Figure 4. For each dynamic CT dataset, the

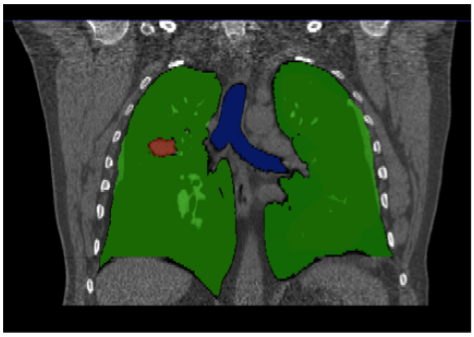

Fig. 4: Tumour volume (red) was segmented manually via ITK-SNAP software.

tumour volume (point cloud) was extracted from the whole image using the associated label and its 3D coordinates. This was repeated to acquire the tumour volume in all phases as a 3D point cloud coordinates (x, y, z). Then the tumour centre of gravity was extracted. Figure 5 illustrates lung tumour centre of gravity motion during respiration for a single patient.

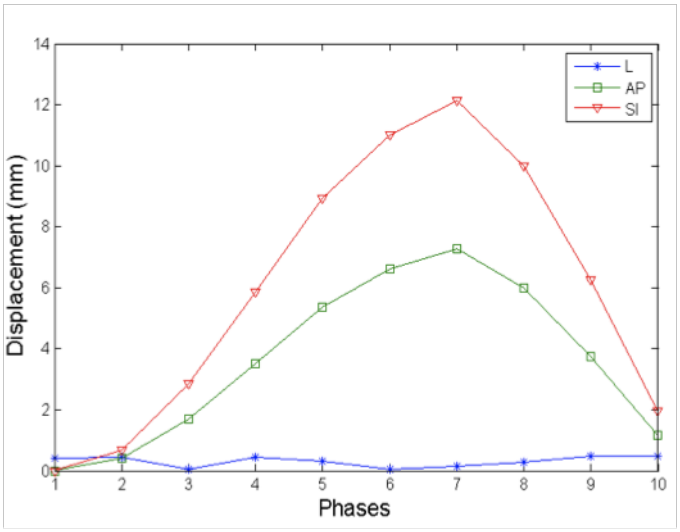

Fig. 5: The Superior-Inferior (SI) (red), Anterior-Posterior (AP) (green) and Lateral (L) (blue) motion of the tumour centre of gravity.

E. Canonical Correlation Analysis

CCA expresses the relationship between the external thoracic and abdomen surface motions ($\mathbf{s^{(T)}}$ and $\mathbf{s^{(A)}}$) and the tumour motion $\mathbf{t}$ in terms of their cross-covariance matrices. CCA can be used in this case to obtain two sets of basis vectors: $\mathbf{u}$ (for tumour) and $\mathbf{v}$, where $\mathbf{v}$ corresponds to thoracic ($\mathbf{v}^{(T)}$) or abdominal ($\mathbf{v}^{(A)}$) motion such that the correlation between the projections of data on these directions is maximized [10]. These basis vectors are acquired through maximizing their correlation.

The original data is then projected to these basic vector by:

$$s_{CCA} = \mathbf{v}^T * \mathbf{s}, \mathbf{t}_{CCA} = \mathbf{u}^T * \mathbf{t}, \quad (2)$$

where $C_{\mathbf{s},\mathbf{s}}$ and $C_{\mathbf{s},\mathbf{t}}$ are the within-set covariance and between-set covariance matrices respectively.

In this primary investigation, the average value of the correlation coefficient ρ across all datasets was very high. It has mean 0.87 and standard deviation 0.21.

F. Prediction Models

The anterior surface motion was predicted using two different methods; AKDE and GMR. Their performances were compared. Let $\xi = (X, \hat{X})$ be the training set composed of N data points / time of D dimensions where X corresponds to the external surface trajectory and $\hat{X}$ represents the external surface velocity. The joint pdf and probability of a datapoint being in a GMM of K Gaussians are calculated using AKDE [1] and GMR [11] respectively. After predicting the highest likelihood of future position of the anterior surface, the tumour's future position is estimated using the CCM model at any anterior position. For each datasets a leave one-out method was applied to validate the proposed algorithm. Table II summaries the results of the correlation-prediction model. The average error has mean 0.44 and standard deviation 0.25 in AKDE and mean 0.84 and standard deviation 0.07 in GMR respectively.

TABLE II: The RMS results of the patient-specific correlation-prediction models in AKDE and GMR.

Data	RMSE (mm) AKDE	RMSE (mm) GMR
1	0.50	0.93
2	0.27	0.84
3	0.63	0.73
4	0.28	0.73
5	1.05	0.94
6	0.44	0.89
7	0.27	0.85
8	0.22	0.82
9	0.30	0.82
Ave.	0.44	0.84
ST	0.25	0.07

III. DISCUSSION AND CONCLUSION

A method to predict the internal target position has been presented. By predicting the position of the anterior patient surface CCA can be utilized to correlate for example markerless external surface motion with internal target position. Comparison of the performance of AKDE versus GMR suggests

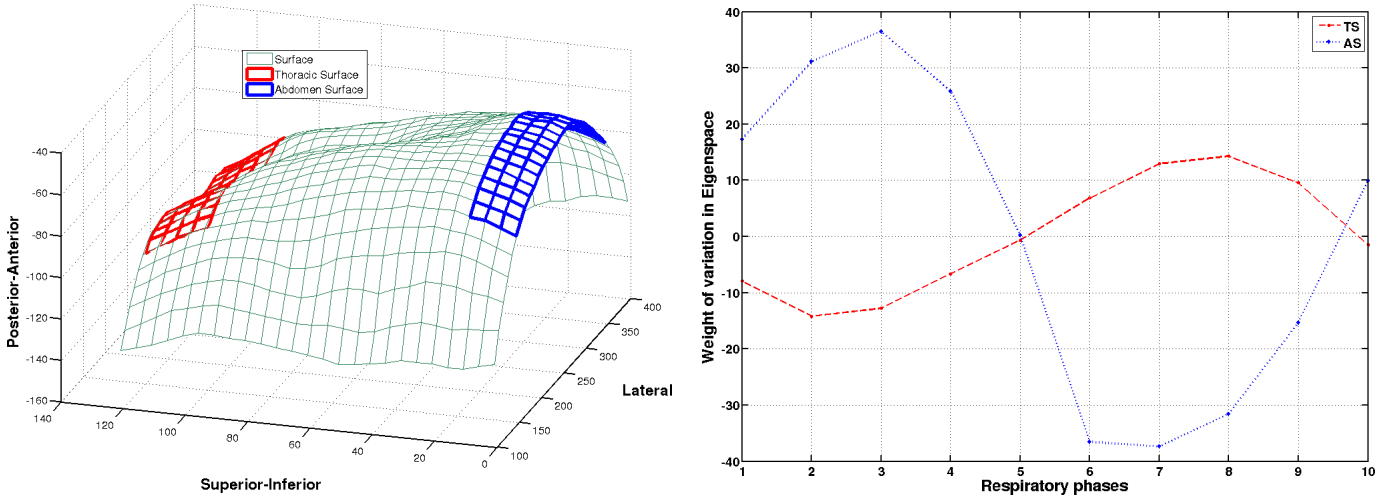

(a) (b)

Fig. 3: (a) The thoracic and abdomen sections of torso surface (b) The extracted respiratory surface motion for thoracic and abdomen sections projected to the first eigenvector.

that the AKDE model has increased performance within the limits of this datasets. The preliminary results of correlation-prediction model indicate a considerably high correlation between the external surface motion and the lung tumour motion and less than $1mm$ accuracy for predicting the internal target obtained. A minimum of $3mm$ margin is added around the tumour in the planning target volume to account for intra/inter motion. So, obtaining about $1mm$ accuracy can reduce this margin and thus potentially save healthy tissue from unwanted irradiation.

ACKNOWLEDGMENT

We would like to thank the the Centre for Vision, Speech and Signal Processing, University of Surrey for providing the funding for this work.

REFERENCES

[1] M. Alnowami, E. Lewis, and K. Wells, "Internal motion prediction using kernel density estimation and general canonical correlation model," in *Nuclear Science Symposium and Medical Imaging Conference (NSS/MIC), 2011 IEEE*, oct. 2011, pp. 3772 –3776.

[2] C. Shi and N. Papanikolaous, "Tracking versus gating in the treatment of moving targets," *European oncological disease*, 2007.

[3] W. Bai and M. Brady, "Motion correction and attenuation correction for respiratory gated pet images," *Medical Imaging, IEEE Transactions on*, vol. 30, no. 2, pp. 351 –365, feb. 2011.

[4] P. J. Keall, G. S. Mageras, J. M. Balter, R. S. Emery, K. M. Forster, S. B. Jiang, J. M. Kapatoes, D. A. Low, M. J. Murphy, B. R. Murray, C. R. Ramsey, M. B. V. Herk, S. S. Vedam, J. W. Wong, and E. Yorke, "The management of respiratory motion in radiation oncology report of aapm task group 76," *Medical Physics*, vol. 33, no. 10, pp. 3874–3900, 2006. [Online]. Available: http://link.aip.org/link/?MPH/33/3874/1

[5] U. Topal and B. Ediz, "Transthoracic needle biopsy: factors effecting risk of pneumothorax," *European Journal of Radiology*, vol. 48, no. 3, pp. 263 – 267, 2003. [Online]. Available: http://www.sciencedirect.com/science/article/pii/S0720048X03000585

[6] A. S. Beddar, K. Kainz, T. M. Briere, Y. Tsunashima, T. Pan, K. Prado, R. Mohan, M. Gillin, and S. Krishnan, "Correlation between internal fiducial tumor motion and external marker motion for liver tumors imaged with 4d-ct," *International Journal of Radiation Oncology*Biology*Physics*, vol. 67, no. 2, pp. 630 – 638, 2007. [Online]. Available: http://www.sciencedirect.com/science/article/pii/S0360301606032391

[7] P. A. Yushkevich, J. Piven, H. Cody Hazlett, R. Gimpel Smith, S. Ho, J. C. Gee, and G. Gerig, "User-guided 3D active contour segmentation of anatomical structures: Significantly improved efficiency and reliability," *Neuroimage*, vol. 31, no. 3, pp. 1116–1128, 2006.

[8] J. Vandemeulebroucke, S. Rit, J. Kybic, P. Clarysse, and D. Sarrut, "Spatiotemporal motion estimation for respiratory-correlated imaging of the lungs," *Medical Physics*, vol. 38, no. 1, pp. 166–178, 2011. [Online]. Available: http://link.aip.org/link/?MPH/38/166/1

[9] E. Castillo, R. Castillo, J. Martinez, M. Shenoy, and T. Guerrero, "Four-dimensional deformable image registration using trajectory modeling," *Physics in Medicine and Biology*, vol. 55, no. 1, p. 305, 2010. [Online]. Available: http://stacks.iop.org/0031-9155/55/i=1/a=018

[10] H. Hotelling, "Relations between two sets of variates," *Biometrika*, vol. 28, no. 3/4, pp. 321–377, 1936. [Online]. Available: http://www.jstor.org/stable/2333955

[11] S. Calinon, *Robot Programming by Demonstration: A Probabilistic Approach*, 1st ed. EFPL Press, August 2009. [Online]. Available: http://www.amazon.com/Robot-Programming-Demonstration-Sylvain-Calinon/dp/1439808678